

This document is confidential and is proprietary to the American Chemical Society and its authors. Do not copy or disclose without written permission. If you have received this item in error, notify the sender and delete all copies.

Systematic screening of deep eutectic solvents as sustainable separation media exemplified by the CO₂ capture process

Journal:	<i>ACS Sustainable Chemistry & Engineering</i>
Manuscript ID	sc-2020-02490c.R1
Manuscript Type:	Article
Date Submitted by the Author:	n/a
Complete List of Authors:	Song, Zhen; Max-Planck-Institut für Dynamik komplexer technischer Systeme, process systems engineering Hu, Xutao; East China University of Science and Technology, Chemical engineering Wu, Hongyi; Otto-von-Guericke-University Magdeburg Faculty of Process and Systems Engineering Mei, Mingcan; East China University of Science and Technology, School of Chemical Engineering Linke, Steffen; Otto von Guericke Universität Magdeburg, Chair for Process Systems Engineering Zhou, Teng; Max-Planck-Institut für Dynamik komplexer technischer Systeme, Qi, Zhiwen; East China University of Science and Technology, State Key Lab of Chemical Engineering Sundmacher, Kai; Max-Planck-Institut für Dynamik komplexer technischer Systeme, Process Systems Engineering

SCHOLARONE™
Manuscripts

Systematic screening of deep eutectic solvents as sustainable separation media exemplified by the CO₂ capture process

Zhen Song,^{a,b} Xutao Hu,^c Hongyi Wu,^a Mingcan Mei,^c Steffen Linke,^a Teng Zhou,^{a,b}
Zhiwen Qi,^c and Kai Sundmacher^{a,b}

^aProcess Systems Engineering, Otto-von-Guericke University Magdeburg, Universitätsplatz 2, D-39106
Magdeburg, Germany

^bProcess Systems Engineering, Max Planck Institute for Dynamics of Complex Technical Systems,
Sandtorstr. 1, D-39106 Magdeburg, Germany

^cSchool of Chemical Engineering, East China University of Science and Technology, 130 Meilong Road,
200237, Shanghai, China

Corresponding author: songz@mpi-magdeburg.mpg.de (Z. S.)

ABSTRACT

Although deep eutectic solvents (DESs) have attracted significant interest in various separation processes, rational methods guiding task-specific DES selection are still scarce. In this work, a systematic method for screening DESs as sustainable separation solvents is proposed and exemplified by the CO₂ capture application. To achieve a large screening space, experimentally reported DESs are collected exhaustively from literature; for the most studied choline chloride (ChCl) based DESs a correlation between their freezing point depression and COSMO-RS molecular descriptors of their hydrogen bond donors (HBDs) is established, which is applied to search a huge number of novel combinations of ChCl and HBD candidates for potential DESs. From the extended database combining experimental and potential DESs, promising CO₂ absorbents are screened by integrating (a) the freezing point constraint according to the operating requirement, (b) the estimation of environment, health, and safety (EHS) impacts using quantitative structure-activity relationships methods, and (c) the prediction of thermodynamic properties by COSMO-RS. The practical solvent performance of the top DES candidates is finally studied by experiments, identifying ChCl: ethylenecyanohydrin (at mole ratios of 1:2 and 1:3) as very attractive CO₂ absorbents.

KEYWORDS: deep eutectic solvent; freezing point depression correlation; EHS impact estimation; COSMO-RS; CO₂ capture

INTRODUCTION

Deep eutectic solvents (DESs) refer to systems obtained from mixing Lewis or Brønsted acids and bases, which present a much lower freezing point (T_f) than either of each individual component.¹ Typical DESs are formed from an organic salt (e.g., ammonium or phosphonium salt) as hydrogen bond acceptor (HBA), and hydroxyl-, carboxyl-, or amino-containing organic alcohols or acids as hydrogen bond donor (HBD).² In contrast to volatile organic compounds, DESs possess many attractive properties such as negligible vapor pressure, broad liquidus range, and easily tunable character, which render them as ionic liquid (IL) analogues. More interestingly, such mixture solvents offer two potential advantages over ILs: (1) in many cases, these solvents can be prepared by simply mixing their components in an appropriate ratio under mild heating, and thus avoid complex synthesis and purification steps as normally required for preparing ILs; (2) a large number of cheap and renewable compounds can be utilized as HBAs or HBDs of DESs, making this spectrum of solvents more affordable and sustainable.¹⁻³ For these reasons, DESs have been recently thrust into the limelight as neoteric solvents for many separation processes, including gas absorption,⁴⁻⁶ liquid-liquid extraction,⁷⁻¹⁰ and natural product purification.¹¹⁻¹³

Of central importance to realize a technically and economically feasible DES-based separation process is the selection of a suitable DES. Most previous studies relied on the experimental test of different combinations of DES components. However, this method is not only expensive and time-consuming, but also cannot ascertain the optimal DES system as a large variety of potential components and their different ratios theoretically result in an almost limitless solvent space. Several groups have utilized equations of state methods such as PC-SAFT for modelling the phase behaviors of DES-containing systems.^{14,15} Nevertheless, these methods require a number of molecule-specific and mixing parameters fitted from experimental data, presenting a limited predictive capability for novel systems. Additionally,

1
2
3 ab initio methods such as molecular dynamics and quantum chemical calculations have also
4
5 been applied to offer useful insight into DES properties and their performances for certain
6
7 separation tasks.^{16,17} However, such methods are highly expertise-dependent and
8
9 computation-demanding, and are thus impractical for extensive DES screening. In this context,
10
11 reliable methods that can guide the efficient screening of DESs are highly desirable.
12

13
14 Compared with the cases for conventional organic solvents and ILs,¹⁸⁻²² the theoretical
15
16 screening or design of DESs for separations is still in its infancy. Hitherto, there are only a
17
18 few DES screening studies which utilize the COSMO-RS method to fast evaluate the
19
20 thermodynamic performances of a number of DESs. Bezold et al. employed COSMO-RS to
21
22 screen DES-based solvent systems, that is, the stationary phase and mobile phase for
23
24 chromatographic separation; the liquid-liquid equilibria of {alkane + alcohol + DES} systems
25
26 are first calculated, and thereafter the partition coefficients of different target solutes in the
27
28 biphasic systems are estimated.^{24,25} Hadj-Kali and coworkers performed the DES screening
29
30 for the denitrification of diesel and the cyclohexane-benzene separation by estimating the
31
32 selectivity, capacity, and performance index at infinite dilution with COSMO-RS.^{26,27} In
33
34 addition to these screening-oriented studies, several researchers also employed the COSMO-
35
36 RS model for predicting and interpreting the thermodynamic properties of certain DESs
37
38 and/or DES-involved mixtures.²⁸⁻³⁵ For instance, Aissaoui et al. evaluated four DESs for the
39
40 dehydration of natural gas and interpreted the structural combination and water absorption
41
42 mechanism combining the activity coefficient prediction, the σ -profile and σ -potential
43
44 analyses using COSMO-RS;²⁸ recently, the research group has integrated the COSMO-RS
45
46 and molecular dynamic methods to study the CO₂ solubility in seven DESs.²⁹ Liu et al.
47
48 evaluated and calibrated COSMO-RS for the prediction of CO₂ solubility in DESs based on
49
50 experimental data, and analyzed the CO₂ absorption mechanism of DESs from analyzing the
51
52 σ -profiles and interaction energies.³⁵ Despite the progress made, these above studies in
53
54
55
56
57
58
59
60

1
2
3 general only covered a small number of DES candidates that are either experimentally
4 reported or hypothetically combined from widely used HBAs and HBDs (presuming their
5 DES formation). In this sense, there is an urgent need for the development of DES screening
6 method to be able to reasonably search optimal candidates over a much larger molecular
7 space.
8
9

10
11
12
13
14 Besides suffering from a limited solvent search space, the previous screening studies also
15 have not specifically considered the environmental, health, and safety (EHS) impacts of DES
16 candidates. This is the case for many experimental DES studies as well, where the possible
17 DES formation of different components and the application performance are mainly
18 concentrated on while the EHS compatibility of DESs is usually taken for granted. However,
19 such assumption is clearly unwarranted, especially when the DESs are not based on natural
20 and sustainable components.³⁶ For instance, Wen et al. studied the biodegradability of eight
21 DESs, out of which only three show a theoretical oxygen demand of 60% or higher within 14
22 days (a general biodegradable threshold);³⁷ several groups have also experimentally proved
23 the toxicity and cytotoxicity of DESs.³⁶ Therefore, to fulfill the potential of DESs as
24 sustainable separation media, it is highly preferable to evaluate the EHS impacts of DESs in
25 the early screening stage.
26
27
28
29
30
31
32
33
34
35
36
37
38
39

40 Taking account of the aforementioned aspects, a systematic method for screening DESs as
41 separation solvent is proposed in the present work (see Figure 1 for the overall framework).
42 The whole DES screening method consists of three main steps. The first step is the DES
43 database collection and extension, aiming to overcome the limited solvent search space in
44 previous DES screening. The experimentally reported DESs are exhaustively collected from
45 literature, based on which a correlation between the freezing point depression (ΔT_f) of DESs
46 and the quantum chemical molecular descriptors of their components is explored for solvent
47 database extension. The next step is the DES screening for a given separation task, which
48
49
50
51
52
53
54
55
56
57
58
59
60

1
2 particularly evaluates the potential EHS impacts of DESs in addition to their thermodynamic
3 properties. In the third step, experiments are carried out to validate the separation
4 performances of the top candidates screened above. To demonstrate the proposed DES
5 screening method, the CO₂ capture process is taken as an illustrative case study.
6
7
8
9
10

11 12 13 **DES DATABASE COLLECTION AND EXTENSION**

14 15 **Collection of experimentally reported DESs**

16
17
18
19
20
21
22
23
24
25
26
27
28
29
30
31
32
33
34
35
36
37
38
39
40
41
42
43
44
45
46
47
48
49
50
51
52
53
54
55
56
57
58
59
60
DESs that have been experimentally reported are collected exhaustively from literature for two purposes: (1) such already existing ones can be first stored as a subset of the final database for DES screening; (2) through analyzing the data on these DESs, prediction methods for the eutectic behaviors between different components could be explored so that one can subsequently search over a larger space of novel HBA: HBD combinations for potential DESs.

As tabulated in Table S1 (Supporting Information), 461 experimentally reported DESs are collected after an exhaustive literature review (in this work, each unique combination of components and component ratios is treated as a distinct DES from the solvent screening point of view). To our best knowledge, this is the largest DES database available up to now. However, comparing with the huge variety of possible HBA: HBD combinations, the already covered ones are only the tip of the iceberg, which clearly highlights the importance of DES database extension. By reviewing the HBAs and HBDs separately, a majority of these collected DESs belong to the type III (i.e., a combination of a quaternary ammonium salt and an HBD) while a notable number of them formed by two non-salt compounds are out of the four types as classified by Smith et al.³ Overall, there are 80 HBAs and 142 HBDs involved for the 461 collected DESs (Table S2, Supporting Information). These HBAs and HBDs could be taken directly as candidate component pools for DES database extension.

ΔT_f prediction of ChCl-based DESs

The core issue for extending DES screening space is to determine whether a novel HBA:HBD combination can potentially present a eutectic behavior with T_f satisfying the operating requirement for a specific task.³⁸ To this end, the most straightforward way is the prediction of solid-liquid equilibria (SLE).^{39,40} By quantifying the SLE curves (as illustrated in Figure 2), one can identify the T_f of the HBA:HBD mixture at different molar ratios, including the eutectic point (T_e) at the eutectic composition (x_e). However, the SLE prediction of DES systems is challenging because it requires experimental properties of components including melting temperature and enthalpy as well as an activity coefficient model for the liquid phase, which are often unavailable for potential DES components of interest. An expedient way to estimate the eutectic behavior between two components could be the prediction of freezing point depression (ΔT_f).³ As shown in Figure 2, ΔT_f denotes the difference between the ideally interpolated temperature at x_e ($T_{f,im}$) and the practical T_e . Once the ΔT_f for a given combination of components is predictable, its T_e can be in turn estimated with the knowledge of the T_f of components (i.e., $T_{f,A}$ and $T_{f,B}$) and the x_e . The T_e of one HBA:HBD combination, which is the lowest T_f it can reach, can be used to primarily check its applicability as solvent for a specific separation.

As the ΔT_f of DESs is generally believed to be positively related to the interactions (often through hydrogen bond) between components,³ Abbott et al. have recently proposed a ΔT_f correlation with the enthalpy of hydrogen bond formation (ΔH_{hb}) on the basis of 13 choline chloride (ChCl) based DESs.⁴¹ However, the obtained correlation could not be applied for general ΔT_f prediction since the experimentally measured ΔH_{hb} is required while the correlation result is yet unsatisfying. From the predictive point of view, it is highly desirable to develop ΔT_f models based on experimentally independent molecular descriptors and possessing better correlation performance. In this work, the third hydrogen bond (HB)

1
2
3 moments HB_acc3 and HB_don3 in the COSMO-RS theory, which are important quantitative
4
5 measures of HB acceptor and donor capacities of compounds,^{42,43} are introduced as molecular
6
7 descriptors associated with HB interaction; moreover, to account for the potential spatial
8
9 factor affecting HB formation,^{41,44} the descriptor of molecular volume is also considered. All
10
11 these HB- and volume-related molecular descriptors of DES components can be readily
12
13 obtained from COSMO-RS analysis. To explore whether such molecular descriptors can be
14
15 applied for a more reliable ΔT_f correlation, the ΔT_f of the experimentally reported DESs are
16
17 exhaustively retrieved. It is found that only a small portion of the DES studies have provided
18
19 the SLE between DES components for ΔT_f determination and most of these DES systems are
20
21 based on the HBA of ChCl.^{1,41,44-48} For this reason, this work only explores the ΔT_f correlation
22
23 with the COSMO-RS (implemented in COSMOthermX16) derived molecular descriptors for
24
25 ChCl-based DESs in the following.
26
27

28
29 As summarized in Table S3 (Supporting Information), there are overall 35 different ChCl-
30
31 based DESs whose ΔT_f can be determined from experimental SLE. Considering the HBAs in
32
33 these DESs are identical, only the molecular descriptors of HBDs are tested for the ΔT_f
34
35 correlation. Based on a randomly selected regression set (31 data points), the best ΔT_f
36
37 correlation is obtained as a multilinear relationship (MLR) with the HB_don3, HB_acc3, and
38
39 molecular volume (V_{COSMO}) of HBDs:
40
41

$$\Delta T_f = 9.03 \times \text{HB_don3} + 2.90 \times \text{HB_acc3} - 0.23 \times V_{\text{COSMO}} + 136.02 \quad (1)$$

42
43
44 The detailed statistical result of this MLR is tabulated in Table 1 and compared with other
45
46 model options in Table S4 (Supporting Information). As seen, (1) all the three descriptors
47
48 have a high F-value and a low p-value (<0.05), confirming that they all have great
49
50 significance in the correlation; (2) the coefficient of determination (R^2) of the above MLR is
51
52 0.85 (much higher than the ΔH_{hb} -based result⁴¹) with a close adjusted R^2 of 0.83; (3) the
53
54 variance inflation factor (VIF) analysis shows negligible multicollinearity between these three
55
56
57

1
2
3 descriptors. From the coefficients of each term, the HB_don3 and HB_acc3 of HBD have a
4 positive effect whereas its V_{COSMO} has a negative effect on the ΔT_f of DES. This good
5 correlation between ΔT_f and the selected molecular descriptors of HBDs essentially validates
6 the significance of HB in the formation of many DESs. Figure 3 compares the MLR
7 correlated and experimentally determined ΔT_f of these ChCl-based DESs. As seen, although
8 the four ChCl-based DESs in the validation set are not used for correlating the MLR, the
9 predicted ΔT_f of them agrees reasonably with their experimental data, demonstrating the
10 reliability of the obtained MLR. Moreover, the broad range of different HBD types (such as
11 urea, phenols, fatty alcohols, sugars, mono- and poly-carboxylic acids) covered by the 35
12 DESs indicates a good generalization ability of the MLR for ΔT_f correlation.

13
14 It is also worth mentioning that the HB_don3, HB_acc3, and V_{COSMO} are empirically selected
15 from different types of COSMO-RS derived molecular descriptors according to the potential
16 mechanism of ΔT_f . However, when other larger descriptor datasets such as all the HB
17 moments⁴² or the area descriptors of the screening charge density (σ -profile)^{49,50} are tested
18 (supported by the principle component analysis or partial least squares method), the best ΔT_f
19 correlation performances are almost at the same level as the present MLR; this finding also
20 holds true if the nonlinear terms between HB_don3, HB_acc3, and V_{COSMO} are tested in the
21 correlation (Table S4, Supporting Information). These comparisons clearly demonstrate the
22 rationality of the selected parameters for correlating the HB-related property of ΔT_f .
23 Considering the remarkable simplicity and mechanism basis, the MLR based on HB_don3,
24 HB_acc3, and V_{COSMO} is thus presented here.

25 26 27 **Searching of potential ChCl-based DESs**

28
29 As already mentioned, the 461 experimentally reported DESs in Table S1 (Supporting
30 Information) are still far less than the large number of possible HBA: HBD combinations.
31 Therefore, from the screening point of view, it is highly desirable to extend the solvent
32
33
34
35
36
37
38
39
40
41
42
43
44
45
46
47
48
49
50
51
52
53
54
55
56
57
58
59
60

1
2
3 database by including more potential DESs. For this purpose, the above MLR model for ΔT_f
4
5 is employed to estimate the eutectic behavior for a large number of novel combinations of
6
7 ChCl with HBD candidates, thereby searching for potential ChCl-based DESs. In this work,
8
9 all the HBDs involved in the experimentally reported DESs (Table S2, Supporting
10
11 Information) and the conventional molecules in COSMObase (Ver. 1301, COSMOlogic
12
13 GmbH) are initially taken as the HBD candidate database, resulting in 7666 novel HBDs to be
14
15 evaluated (Table S5, Supporting Information). Of course, one can introduce other molecular
16
17 databases if more potential HBDs are desired for the DES database extension.
18
19

20
21 To screen out promising HBDs of ChCl-based DESs, two sets of empirical constraints are
22
23 considered prior to the ΔT_f estimation. First, to ensure a selected compound can practically act
24
25 as HBD, a lower bound on the HB_don3 and an upper bound on the HB_acc3 are introduced.
26
27 By analyzing the 35 experimentally reported ChCl-based DESs, this work sets these values as
28
29 1.63 and 12.61, respectively. With these bounds, candidates with poor HB donor capacity or
30
31 mainly featuring HB acceptor capacity could be discarded. Correspondingly, 1691 HBD
32
33 candidates in the initial database are retained. Second, the boiling points of HBD candidates
34
35 are constrained to be higher than 373.15 K, thereby eliminating the highly volatile candidates
36
37 that are not favorable from the perspective of facile preparation, operation safety, and thermal
38
39 stability of potential DESs. Consequently, 1390 of the 1691 HBD candidates survived.
40
41 Among the discarded candidates, some potential ones may be missed by these rigorous
42
43 empirical constraints. With more understanding of DES properties in the future, such
44
45 empirical constraints could be properly modified in the pre-screening.
46
47
48

49
50 Following the empirical pre-screening, the ΔT_f of the combinations of ChCl with each of the
51
52 1390 remaining HBDs is estimated by the MLR model (that is, 1390 ChCl: HBD
53
54 combinations without considering the component ratios). However, as mentioned above, it is
55
56 the T_e rather than the ΔT_f that primarily determines the applicability of an HBA: HBD
57
58

1
2
3 combination as solvent for a specific separation.³⁸⁻⁴⁰ Therefore, the T_e is further evaluated for
4
5 the 1390 ChCl: HBD combinations. In the case of different ChCl: HBD combinations, the T_f
6
7 of ChCl is known (575.15 K) and those of HBD candidates can be obtained from either the
8
9 COSMObase or other online databases (e.g., PubChem). Regarding the x_e , there is still no
10
11 reliable prediction method. However, it is found that all the 35 experimentally reported DESs
12
13 based on ChCl have the molar ratio of HBA to HBD not higher than 1:1 (12 of 1:1, 2 of 1:1.5,
14
15 18 of 1:2, and 3 of 1:3).^{1,41,44-48} Considering that the T_f of components and the ΔT_f are fixed
16
17 for a given HBA: HBD combination while ChCl has a higher T_f than almost all the 1390 HBD
18
19 candidates, the larger HBA to HBD molar ratio at the x_e will lead to a higher T_e . Thus, the
20
21 maximum eutectic points (T_{me}) of different ChCl: HBD combinations can be estimated by
22
23 assuming their x_e at the HBA: HBD molar ratio of 1:1 (as shown in Figure 2). The T_{me} can be
24
25 used instead of T_e to check whether a ChCl: HBD combination can satisfy the operating
26
27 temperature requirement for a specific separation process in DES screening. Table S6
28
29 (Supporting Information) ranks the 1390 ChCl: HBD combinations in the increasing order of
30
31 their T_{me} . From the table, one can readily identify a list of potential DESs according to
32
33 different tasks, which can be combined with the experimentally reported DESs as an extended
34
35 database for solvent screening.
36
37
38
39
40
41

42 **DES SCREENING**

43
44
45 In this section, the CO₂ capture process is employed as a case study to illustrate the DES
46
47 screening procedure for separation tasks. This process has been intensively studied in the past
48
49 decades since CO₂ is regarded as the most significant anthropogenic greenhouse gas and the
50
51 major contributor to global warming.^{6,51} A number of studies have recently reported the CO₂
52
53 solubility in DESs whereas extensive DES screening work on this process is yet scarce.⁵²⁻⁵⁷
54
55
56
57
58
59
60

Screening by T_f constraint

To obtain DESs that can be applied as room temperature CO₂ absorbent, all the candidates in the combined database of Tables S1 and S6 (Supporting Information) are first screened by imposing a T_f constraint of below 298.15 K. As a result, 241 of the 461 experimental DESs are retained, which are reported either having a T_f lower than 298.15 K or being liquid state at room temperature. Meanwhile, 158 of the 1390 potential ChCl: HBD combinations satisfy the T_f constraint as they have a T_{me} lower than 298.15 K. The screened DES candidates in this step are tabulated in Table S7 (Supporting Information).

Screening by EHS impacts

To realize the potential of DESs as sustainable solvents, the EHS impacts of DESs are further considered after the screening by T_f . As there is still no predictive method for the EHS impacts of DESs, such properties are estimated empirically from those of their individual components.

Regarding the HBDs involved in the DES candidates, the modern software package VEGA⁵⁸ is first employed to evaluate five molecular properties concerning EHS: the persistence, the bioconcentration factor (BCF), mutagenicity, carcinogenicity, and toxicity. VEGA is a computational platform that incorporates a series of quantitative structure-activity relationship (QSAR) models for EHS-related properties of molecules. Simply inputted with the SMILES of molecules, these QSAR models can give the prediction on the EHS-related properties along with a reliability measure of the corresponding prediction. Generally, the prediction reliability of these models is divided into four levels namely experimental (i.e., experimental data available), good, moderate, and low, which is assessed from the applicability domain index for each prediction. For each of the five concerned properties, there is more than one QSAR method available in VEGA; this work selects all of them and their predictions are integrated to make the overall assessment. To be specific, by integrating the prediction result and

1
2
3 reliability of different available models, each EHS-related property is classified into five
4
5 grades as follows.

6
7 Grade 1 (green): consistent predictions obtained by different models with good reliability
8
9 or experimental data available for negative result;

10
11 Grade 2 (purple): consistent predictions obtained by different models with only moderate
12
13 or low reliability for negative result;

14
15 Grade 3 (blue): inconsistent predictions obtained by different models while negative
16
17 result is obtained with good reliability by at least one model;

18
19 Grade 4 (yellow): inconsistent predictions obtained by different models while no
20
21 negative result is obtained with good reliability by any model;

22
23 Grade 5 (red): consistent predictions obtained by different models or experimental data
24
25 available for positive result.

26
27 In the above grades, the negative result refers to non-persistent, non-bioaccumulative, non-
28
29 mutagenic, non-carcinogenic and non-toxic, respectively, whereas the positive result indicates
30
31 the opposites.
32
33

34
35 For the overall 242 HBDs involved in the remaining DES candidates (Table S7, Supporting
36
37 Information), the prediction results of the five properties by different QSAR models are
38
39 detailed in Table S8 (Supporting Information). The grade table of the five properties for these
40
41 HBDs is summarized in Table S9 (Supporting Information) and shown in Figure 4 with some
42
43 representatives. In this work, the HBDs are considered to be potentially EHS-compatible only
44
45 when all the five concerned properties are in the first three grades (marked in green, purple or
46
47 blue) and otherwise are discarded. Correspondingly, 73 out of the 242 involved HBDs
48
49 survived. To finally identify whether these 73 HBDs could be utilized as EHS-compatible
50
51 DES components, they are further gone over in the PubChem database to eliminate other
52
53 potential concerns such as flammability, air- and water-sensitivity. As a consequence, 56 of
54
55
56
57

1
2
3 the 73 HBDS are retained.

4
5 For the salt HBAs involved in the DES candidates, the VEGA software is inapplicable
6
7 because such salt-like compounds are generally not included for training the incorporated
8
9 QSAR models.⁵⁸ Therefore, only the EHS-impacts of non-salt HBAs, such as betaine,
10
11 menthol, and *N*-methylacetamide are estimated (also seen in Tables S8 - S9, Supporting
12
13 Information). Besides, ChCl, the most prevailing salt HBA, is known as an extensively used
14
15 pro-vitamin in food and other consumer products and has merits such as low cost and
16
17 economic synthesis.^{39,48} Hence, ChCl is also selected as an EHS-compatible HBA. The other
18
19 involved salt HBAs are not considered subsequently in this work due to their yet uncertain
20
21 EHS properties.
22
23

24
25 By estimating the EHS properties of individual components as above, 36 experimentally
26
27 reported DESs and 35 potential ChCl: HBD combinations are screened in this step with
28
29 promising EHS-compatibility (Table S10, Supporting Information).
30
31

32 **Screening by thermodynamic properties**

33 *Fundamentals of thermodynamic screening*

34
35 Of central relevance to select DESs as separation solvent is predicting the thermodynamic
36
37 properties of DES-containing systems. In this step, the COSMO-RS model is taken for this
38
39 purpose as it has been demonstrated to deliver good qualitative and in some cases acceptable
40
41 quantitative predictions on the activity coefficient of different solutes in DESs and phase
42
43 equilibria of DES-containing systems such as {DES + alcohol/aromatic/sulfur- or nitrogen-
44
45 compound + alkane}.²⁴⁻³⁵ Considering the introduction of the model is elaborated elsewhere,⁴²
46
47 only the main features for understanding the prediction in this work are briefly addressed as
48
49 follows.
50
51
52
53

54
55 Beyond characterizing molecules with different molecular descriptors (as used in Section 2),
56
57

COSMO-RS is essentially a model for calculating thermodynamic equilibria of fluids and liquid mixtures. A standard COSMO-RS calculation requires only the σ -profiles of the involved compounds, which details the amount of surface with polarity σ on the surface of a molecule. Based on interacting surfaces combining the σ -profile with a fast and accurate statistical thermodynamic treatment, the chemical potential of compound i in a solvent or solvent mixture S (μ_i^S) can be derived and thus a variety of thermodynamic properties are obtainable. For instance, the Henry's law constant of a given solute j in S (H_j^S) can be calculated as:

$$H_j^S = \frac{(\mu_j^{S,\infty} - \mu_j^{Gas})}{RT} \quad (2)$$

where $\mu_j^{S,\infty}$ and μ_j^{Gas} are the chemical potential of j at infinite dilution in S and in the ideal gas phase, respectively. For incompressible liquid state, H_j^S is equivalent to:

$$H_j^S = \gamma_j^{S,\infty} p_j^0 \quad (3)$$

where $\gamma_j^{S,\infty}$ refers to the infinite dilution activity coefficient of j in S and p_j^0 denotes the vapor pressure of pure solute j .

For the representation of DESs in COSMO-RS, the electroneutral mixture approach is selected as it has been proven to deliver comparable results with other possible approaches while being more convenient for DES screening.^{24,26,27} As an example, for a [cation][anion]:HBD ($m:n$) DES, the COSMO-RS input is m mole of cations, m mole of anions, and n mole of the HBD. In COSMO-RS calculation, all these constituents contribute to the total moles, which differ from the experimental definition (m mole of salt and n mole of HBD). Therefore, COSMO-RS derived properties that depend on the definition of mole fraction have to be converted to ensure the same reference standard as used in experiments. For instance, the Henry's law constant of solute j in the [cation][anion]:HBD ($m:n$) DES derived from

COSMO-RS (H_j^{COSMO}) can be converted to the experimentally based value (H_j^{exp}) as:

$$H_j^{\text{exp}} = \frac{m+n}{2m+n} H_j^{\text{COSMO}} \quad (4)$$

For the CO₂ capture case study, the absorption capacity (AC) and desorption easiness (DE) are employed as the thermodynamic criteria for DES screening, which are derived from the Henry's law constant as:

$$AC = \frac{1}{H_{CO_2}^{298.15}} \times \frac{MW_{CO_2}}{MW_{DES}} \quad (5)$$

$$DE = \frac{H_{CO_2}^{328.15}}{H_{CO_2}^{298.15}} \quad (6)$$

where MW_{CO_2} and MW_{DES} are the molecular weights of CO₂ and DES; $H_{CO_2}^{298.15}$ and $H_{CO_2}^{328.15}$ represent the Henry's law constant of CO₂ in DES at 298.15 K and 328.15 K, respectively. Similar criteria have been demonstrated to be effective for screening ILs with promising mass-based gas absorption performances and thus are also utilized here for DES screening.^{59,60} In the following, all the involved COSMO-RS calculations are performed under the parameterization of BP_TZVP_16.ctd in COSMOthermX16.

Results of thermodynamic screening

Prior to thermodynamic screening, the predictive reliability of COSMO-RS for CO₂-in-DES systems is evaluated by comparing experimentally reported H_{CO_2} with their COSMO-RS predicted counterparts (Table S11, Supporting Information).⁵²⁻⁵⁴ Nine HBA: HBD combinations are involved in the evaluation, covering three different HBAs and seven different HBDs. For these combinations, H_{CO_2} of different HBA: HBD molar ratios (1: 2 – 5) and within a wide temperature range (293.15 K – 323.15 K) are involved. As compared in Figure 5, despite some reasonable deviations, the COSMO-RS predicted H_{CO_2} are in good qualitative agreement with the experimental results, which can be suggested by the relatively

high R^2 (0.83). Moreover, the quantitative prediction performance of COSMO-RS for H_{CO_2} is estimated through the absolute average relative deviation (AARD):

$$AARD = \frac{1}{ND} \sum_1^{ND} \left| \frac{H_{CO_2}^{exp} - H_{CO_2}^{cal}}{H_{CO_2}^{exp}} \right| \quad (7)$$

where $H_{CO_2}^{exp}$ and $H_{CO_2}^{cal}$ are the experimental and calculated H_{CO_2} , respectively; ND is the number of data points. Although the AARD is 43.60% for the H_{CO_2} directly predicted by COSMO-RS, it is notably decreased to 8.65% after calibrated by the linear correlation (see Table S11, Supporting Information). Considering the fully predictive character of COSMO-RS, such a quantitative performance after calibration is quite acceptable, which agrees with the finding based on 502 data of CO_2 solubility. Therefore, the COSMO-RS model assisted by the obtained calibration relationship can be applied as a suitable thermodynamic method for the DES screening for the CO_2 capture case study.

After the COSMO-RS benchmarking, the AC and DE of the DES candidates remained after the EHS screening are predicted by COSMO-RS (combining with the linear calibration). For evaluating the AC and DE of the potential ChCl: HBD combinations, three most common HBA: HBD molar ratios of ChCl-based DESs namely 1:1, 1:2, and 1:3 are tested. Figure 6 shows the obtained AC and DE of the involved DES candidates (see detailed data in Table S12, Supporting Information). As both higher AC and DE are favorable for the CO_2 capture, only the candidates simultaneously ranking top 50% in these two criteria are screened out in this step. The corresponding lower bounds (lb) for the AC and DE are found to be 1.20×10^{-3} and 1.45, respectively. Consequently, 10 experimentally reported and 34 potential ChCl-based DESs are retained in the upper right region in Figure 6. To evaluate their overall suitability for CO_2 capture, the AC and DE of them are multiplied. According to the ranking of $AC \times DE$ (Table 2), only two of the top 10 candidates are experimentally reported DESs while the others are all potential ones first suggested in this work. The much larger number of potential

1
2
3 ChCl-based DESs satisfying the lower bounds for AC and DE (Figure 5) and ranking top in
4 AC × DE (Table 2) demonstrates the significance of searching novel DESs beyond the
5 experimentally reported ones.
6
7
8
9
10

11 **EXPERIMENTAL VALIDATION**

12
13
14 From the above screening, the first DES with the highest AC × DE is ChCl: urea (1:2). This
15 DES has already been experimentally proven to possess higher CO₂ capacity than DESs like
16 ChCl: glycerol (1:2) and ChCl: ethylene glycol (1:2), which are also comparable to some
17 [Bmim]-based ionic liquids paired with anions [PF₆]⁻, [BF₄]⁻, [DCA]⁻, and [Tf₂N]⁻.⁵⁵ Such
18 result could well suggest the reliability of the proposed DES screening method for the case
19 study. Nevertheless, to validate that promising potential ChCl: HBD DESs are also identified,
20 experiments for the ChCl: ethylenecyanohydrin combinations that rank from second to fourth
21 in Table 2, are carried out.
22
23
24
25
26
27
28
29
30
31

32 Before the CO₂ absorption experiments, the ChCl: ethylenecyanohydrin combinations (1:1,
33 1:2, and 1:3) are prepared accordingly. ChCl (≥99 wt%, purchased from Acros) is pretreated
34 under vacuum drying at 80 °C for 24 h before use; ethylenecyanohydrin (≥99 wt%, purchased
35 from Adamas) is used as received. In a typical run, appropriate amounts of ChCl and
36 ethylenecyanohydrin, weighed by a Sartorius BSA224S-CW balance (± 0.0001 g), are mixed
37 according to their molar ratios. The mixture is then heated to 323.15 K and stirred for 3 h to
38 ensure the complete mixing of the two components. Afterwards, the mixture is cooled down
39 to room temperature and inspected visually to check the formation of DESs. Following such a
40 preparation procedure, a clear homogenous liquid is obtained for the ChCl:
41 ethylenecyanohydrin combinations (1:2 and 1:3) whereas a cloudy mixture is observed for the
42 ChCl: ethylenecyanohydrin (1:1). The reason why ChCl: ethylenecyanohydrin (1:1) doesn't
43 form a homogeneous liquid can be understood as follows: for pre-screening potential HBDs
44
45
46
47
48
49
50
51
52
53
54
55
56
57
58
59
60

1
2
3 by the T_f constraint, the T_{me} is estimated by assuming the x_e of ChCl: HBD combinations at
4 the mole ratio of 1:1; however, for a specific ChCl: HBD combination (e.g.; ChCl:
5 ethylenecyanohydrin), it is likely that the practical x_e locates at a smaller molar ratio (<1:1),
6 which will lead to the T_e of the binary system lower than T_{me} but in turn bring about a higher
7 freezing point of the mixture at 1:1 (as illustrated in Figure 2). Subsequently, the CO₂
8 absorption experiments are only performed for the ChCl: ethylenecyanohydrin (1:2 and 1:3).
9
10

11
12
13
14
15
16 The pressure drop method, as introduced elaborately in our earlier work,¹⁷ is employed to
17 determine the CO₂ solubility in the DESs under pressure below 1500 kPa at 298.15 K and
18 328.15 K. The obtained results in molarity and molality are given in Table S13 (Supporting
19 Information). As seen in Figure 7, the CO₂ solubility in the DESs grows almost linearly with
20 increasing pressure and the extrapolation line basically passes through the origin of the
21 coordinate, indicating a physical absorption of CO₂ in these solvents. Moreover, the CO₂
22 solubility in ChCl: ethylenecyanohydrin at the molar ratio of 1:2 is higher than that at the
23 molar ratio of 1:3 under the same conditions and increasing the temperature from 298.15 K to
24 328.15 K notably decreases the CO₂ solubility in both two cases. Such experimental results
25 correspond well to the COSMO-RS derived AC and DE. Based on the measured solubility,
26 the molality based Henry's law constant (H_m) of CO₂ in the two DESs is calculated and
27 compared to those in previously reported DESs⁵²⁻⁵⁷ and in some typical ionic liquids^{61,62} and
28 commercial physical absorbents.⁶³⁻⁶⁵ As seen in Table 3, the H_m of CO₂ in the studied DESs at
29 298.15 K is lower than that in ChCl: urea (1:2), ChCl: glycerol (1:2), and ChCl: ethylene
30 glycol (1:2) at 303.15 K, and is even lower than that in the other HBA: HBD combinations at
31 293.15 K. The low level of H_m of the studied DESs also holds when comparing to the cases of
32 typical ionic liquids and commercial physical absorbents. Such comparisons well demonstrate
33 the satisfactory CO₂ absorption capacity of ChCl: ethylenecyanohydrin (1:2 and 1:3).
34
35
36
37
38
39
40
41
42
43
44
45
46
47
48
49
50
51
52
53
54
55 Combining the potential EHS-compatibility, the DESs identified here are indeed attractive
56
57
58
59
60

1
2
3 CO₂ absorbents. It is worth mentioning that only the three common HBA: HBD molar ratios
4
5 for ChCl-based DESs are tested here for the validation purpose; however, from the
6
7 application point of view, further optimization potential could be expected by fine-tuning the
8
9 molar ratio of this DES.
10

11 12 13 14 **CONCLUSION**

15
16 The systematic screening of DESs as sustainable separation solvent is presented in this work
17
18 taking the CO₂ capture process as an illustrative example. A database of 461 experimentally
19
20 reported DESs is built and a reliable MLR correlation between the ΔT_f of ChCl-based DESs
21
22 and the HB_don3, HB_acc3, and V_{COSMO} of their HBDs is established. Based on the obtained
23
24 ΔT_f correlation, potential ChCl-based DESs are searched over novel combinations with 7666
25
26 HBDs from experimental and COSMO-RS molecular database, which are combined with the
27
28 experimental DESs as an extended database for DES screening. Illustrated by the CO₂ capture
29
30 case study, promising DES candidates are identified after screening by T_f constraint, potential
31
32 EHS impacts, and thermodynamic properties. The top potential DES candidates, ChCl:
33
34 ethylenecyanohydrin (1:2, 1:3), are experimentally demonstrated to have encouraging CO₂
35
36 absorption performance. Beyond the case study, the extended DES database and the screening
37
38 method could be easily applied to support the selection of DESs for other separation
39
40 applications. In future work, with more experimental data available, the ΔT_f correlation model
41
42 can be further extended, for example, to cover other types of HBAs in addition to ChCl,
43
44 thereby enabling the search of more diverse DESs.
45
46
47
48
49
50
51
52
53
54
55
56
57
58
59
60

ASSOCIATED CONTENT

The Supporting Information is available free of charge on the ACS Publications Website at DOI:***.

Experimental DESs database collected from literature; HBAs and HBDs involved in experimental DES database; 35 ChCl-based DESs for ΔT_f correlation; statistical comparison of different model options for ΔT_f ; novel HBDs considered in the initial database; 1390 potential ChCl-based DESs in the increasing order of estimated T_{me} ; DES candidates screened after imposing T_f constraint; predicted EHS-relevant properties for the involved HBDs and HBAs; grade table of the five EHS-relevant properties for the involved HBDs and HBAs; DES candidates screened after EHS impacts estimation; comparison of experimental and COSMO-RS predicted H_x of CO_2 in DESs; predicted AC and DE for DES screening; experimentally determined CO_2 solubility in the studied DESs (XLSX).

ACKNOWLEDGEMENTS

The authors gratefully acknowledge the support of the Sino-German joint research project led by Deutsche Forschungsgemeinschaft (DFG) and National Natural Science Foundation of China (NSFC) under the grants SU 189/9-1 and 21861132019, respectively.

REFERENCE

1. Abbott, A. P.; Boothby, D.; Capper, G.; Davies, D. L.; Rasheed, R. K. Deep eutectic solvents formed between choline chloride and carboxylic acids: versatile alternatives to ionic liquids. *J. Am. Chem. Soc.* **2004**, *126*, 9142-9147.
2. Zhang, Q. H.; Vigier, K. D.; Royer, S.; Jerome, F. Deep eutectic solvents: syntheses, properties and applications. *Chem. Soc. Rev.* **2012**, *41*, 7108-7146.
3. Smith, E. L.; Abbott, A. P.; Ryder, K. S. Deep eutectic solvents (DESs) and their applications. *Chem. Rev.* **2014**, *114*, 11060-11082.
4. Sze, L. L.; Pandey, S.; Ravula, S.; Pandey, S.; Zhao, H.; Baker, G. A.; Baker, S. N. Ternary deep eutectic solvents tasked for carbon dioxide capture. *ACS Sustain. Chem. Eng.* **2014**, *2*, 2117-2123.
5. Zhong, F. Y.; Zhou, L.; Shen, J.; Liu, Y.; Fan, J. P.; Huang, K. Rational design of azole-based deep eutectic solvents for highly efficient and reversible capture of ammonia. *ACS Sustain. Chem. Eng.* **2019**, *7*, 14170-14179.
6. Sarmad, S.; Mikkola, J. P.; Ji, X. Carbon dioxide capture with ionic liquids and deep eutectic solvents: a new generation of sorbents. *ChemSusChem* **2017**, *10*, 324-352.
7. Gilmore, M.; McCourt, E. N.; Connolly, F.; Nockemann, P.; Swadźba-Kwaśny, M.; Holbrey, J. D. Hydrophobic deep eutectic solvents incorporating trioctylphosphine oxide: advanced liquid extractants. *ACS Sustain. Chem. Eng.* **2018**, *6*, 17323-17332.
8. Bezold, F.; Minceva, M. Liquid-liquid equilibria of n-heptane, methanol and deep eutectic solvents composed of carboxylic acid and monocyclic terpenes. *Fluid Phase Equilib.* **2018**, *477*, 98-106.
9. Larriba, M.; Ayuso, M.; Navarro, P.; Delgado-Mellado, N.; Gonzalez-Miquel, M.; García, J.; Rodríguez, F. Choline chloride-based deep eutectic solvents in the dearomatization of gasolines. *ACS Sustain. Chem. Eng.* **2018**, *6*, 1039-1047.
10. Gouveia, A. S.; Oliveira, F. S.; Kurnia, K. A.; Marrucho, I. M. Deep eutectic solvents as azeotrope breakers: liquid-liquid extraction and COSMO-RS prediction. *ACS Sustain. Chem. Eng.* **2016**, *4*, 5640-5650.
11. Abbott, A. P.; Cullis, P. M.; Gibson, M. J.; Harris, R. C.; Raven, E. Extraction of glycerol from biodiesel into a eutectic based ionic liquid. *Green Chem.* **2007**, *9*, 868-872.
12. Rodríguez-Llorente, D.; Bengoa, A.; Pascual-Muñoz, G.; Navarro, P.; Águeda, V. I.; Delgado, J. A.; Álvarez-Torrellas, S.; García, J.; Larriba, M. Sustainable recovery of volatile fatty acids from aqueous solutions using terpenoids and eutectic solvents. *ACS Sustain. Chem. Eng.* **2019**, *7*, 16786-16794.

- 1
2
3 13. Wan Mahmood, W. M. A.; Lorwirachsutee, A.; Theodoropoulos, C.; Gonzalez-Miquel, M.
4 Polyol-Based deep eutectic solvents for extraction of natural polyphenolic antioxidants
5 from chlorella vulgaris. *ACS Sustain. Chem. Eng.* **2019**, *7*, 5018-5026.
6
7
8 14. Pontes, P. V.; Crespo, E. A.; Martins, M. A.; Silva, L. P.; Neves, C. M.; Maximo, G. J.;
9 Hubinger, M. D.; Batista, E.; Pinho, S. P.; Coutinho, J. A.P.; Sadowski, G.; Held, C.
10 Measurement and PC-SAFT modeling of solid-liquid equilibrium of deep eutectic
11 solvents of quaternary ammonium chlorides and carboxylic acids. *Fluid Phase Equilibr.*
12 **2017**, *448*, 69-80.
13
14
15 15. Dietz, C. H.; van Osch, D. J.; Kroon, M. C.; Sadowski, G.; van Sint Annaland, M.;
16 Gallucci, F.; Zubeir, L. F.; Held, C. PC-SAFT modeling of CO₂ solubilities in
17 hydrophobic deep eutectic solvents. *Fluid Phase Equilibr.* **2017**, *448*, 94-98.
18
19
20 20 16. Wagle, D. V.; Zhao, H.; Deakynne, C. A.; Baker, G. A. Quantum chemical evaluation of
21 deep eutectic solvents for the extractive desulfurization of fuel. *ACS Sustain. Chem. Eng.*
22 **2018**, *6*, 7525-7531.
23
24
25 26 17. Wang, J.; Cheng, H.; Song, Z.; Chen, L.; Deng, L.; Qi, Z. Carbon dioxide solubility in
27 phosphonium-based deep eutectic solvents: an experimental and molecular dynamics
28 study. *Ind. Eng. Chem. Res.* **2019**, *58*, 17514-17523.
29
30
31 32 18. Zhou, T.; Song, Z.; Zhang, X.; Gani, R.; Sundmacher, K. Optimal solvent design for
33 extractive distillation processes: a multiobjective optimization-based hierarchical
34 framework. *Ind. Eng. Chem. Res.* **2019**, *58*, 5777-5786.
35
36
37 38 19. Song, Z.; Zhou, T.; Zhang, J.; Cheng, H.; Chen, L.; Qi, Z. Screening of ionic liquids for
39 solvent-sensitive extraction – with deep desulfurization as an example. *Chem. Eng. Sci.*
40 **2015**, *129*, 69-77.
41
42
43 44 20. Liu, X.; Huang, Y.; Zhao, Y.; Gani, R.; Zhang, X.; Zhang, S. Ionic liquid design and
45 process simulation for decarbonization of shale gas. *Ind. Eng. Chem. Res.* **2016**, *55*, 5931-
46 5944.
47
48
49 50 21. Song, Z.; Zhang, C.; Qi, Z.; Zhou, T.; Sundmacher, K. Computer-aided design of ionic
51 liquids as solvents for extractive desulfurization. *AIChE J.* **2018**, *64*, 1013-1025.
52
53
54 55 22. Song, Z.; Hu, X.; Zhou, Y.; Zhou, T.; Qi, Z.; Sundmacher, K. Rational design of double
56 salt ionic liquids as extraction solvents: separation of thiophene/n-octane as example.
57 *AIChE J.* **2019**, *65*, No. e16625.
58
59
60 23. Silva, L. P.; Fernandez, L.; Conceição, J. H.; Martins, M. A.; Sosa, A.; Ortega, J.; Pinho,
S. P.; Coutinho, J. A. Design and characterization of sugar-based deep eutectic solvents

- 1
2
3 using conductor-like screening model for real solvents. *ACS Sustain. Chem. Eng.* **2018**, *6*,
4 10724-10734.
5
6 24. Bezold, F.; Weinberger, M. E.; Minceva, M. Assessing solute partitioning in deep eutectic
7 solvent-based biphasic systems using the predictive thermodynamic model COSMO-RS.
8 *Fluid Phase Equilibr.* **2017**, *437*, 23-33.
9
10 25. Bezold, F.; Weinberger, M. E.; Minceva, M. Computational solvent system screening for
11 the separation of tocopherols with centrifugal partition chromatography using deep
12 eutectic solvent-based biphasic systems. *J. Chromatogr. A* **2017**, *1491*, 153-158.
13
14 26. Hizaddin, H. F.; Ramalingam, A.; Hashim, M. A.; Hadj-Kali, M. K. Evaluating the
15 performance of deep eutectic solvents for use in extractive denitrification of liquid fuels
16 by the conductor-like screening model for real solvents. *J. Chem. Eng. Data* **2014**, *59*,
17 3470-3487.
18
19 27. Salleh, Z.; Wazeer, I.; Mulyono, S.; El-blidi, L.; Hashim, M. A.; Hadj-Kali, M. K.
20 Efficient removal of benzene from cyclohexane-benzene mixtures using deep eutectic
21 solvents–COSMO-RS screening and experimental validation. *J. Chem. Thermodyn.* **2017**,
22 *104*, 33-44.
23
24 28. Aissaoui, T.; AlNashef, I. M.; Benguerba, Y. Dehydration of natural gas using choline
25 chloride based deep eutectic solvents: COSMO-RS prediction. *J. Nat. Gas Sci. Eng.* **2016**,
26 *30*, 571-577.
27
28 29. Alioui, O.; Benguerba, Y.; Alnashef, I. M. Investigation of the CO₂-solubility in deep
29 eutectic solvents using COSMO-RS and molecular dynamics methods. *J. Mol. Liq.* **2020**,
30 *307*, 113005.
31
32 30. Mulyono, S.; Hizaddin, H. F.; Alnashef, I. M.; Hashim, M. A.; Fakeeha, A. H.; Hadj-Kali,
33 M. K. Separation of BTEX aromatics from n-octane using a (tetrabutylammonium
34 bromide + sulfolane) deep eutectic solvent–experiments and COSMO-RS prediction. *RSC*
35 *Adv.* **2014**, *4*, 17597-17606.
36
37 31. Hizaddin, H. F.; Sarwono, M.; Hashim, M. A.; Alnashef, I. M.; Hadj-Kali, M. K.
38 Coupling the capabilities of different complexing agents into deep eutectic solvents to
39 enhance the separation of aromatics from aliphatics. *J. Chem. Thermodyn.* **2015**, *84*, 67-75.
40
41 32. Hadj-Kali, M. K.; Mulyono, S.; Hizaddin, H. F.; Wazeer, I.; El-Blidi, L.; Ali, E.; Ali
42 Hashim, M.; AlNashef, I. M. Removal of thiophene from mixtures with n-heptane by
43 selective extraction using deep eutectic solvents. *Ind. Eng. Chem. Res.* **2016**, *55*, 8415-
44 8423.
45
46
47
48
49
50
51
52
53
54
55
56
57
58
59
60

- 1
2
3 33. Hizaddin, H. F.; Hadj-Kali, M. K.; Ramalingam, A.; Hashim, M. A. Extractive
4 denitrogenation of diesel fuel using ammonium-and phosphonium-based deep eutectic
5 solvents. *J. Chem. Thermodyn.* **2016**, *95*, 164-173.
6
7
8 34. El-hoshoudy, A. N.; Soliman, F. S.; Mansour, E. M.; Zaki, T.; Desouky, S. M.
9 Experimental and theoretical investigation of quaternary ammonium-based deep eutectic
10 solvent for secondary water flooding. *J. Mol. Liq.* *294*, No. 111621.
11
12 35. Liu, Y.; Yu, H.; Sun, Y.; Zeng, S.; Zhang, X.; Nie, Y.; Zhang, S.; Ji, X. Screening deep
13 eutectic solvents for CO₂ capture with COSMO-RS. *Front. Chem.* **2020**, *8*, No. 82.
14
15 36. Clarke, C. J.; Tu, W. C.; Levers, O.; Brohl, A.; Hallett, J. P. Green and sustainable
16 solvents in chemical processes. *Chem. Rev.* **2018**, *118*, 747-800.
17
18 37. Wen, Q.; Chen, J. X.; Tang, Y. L.; Wang, J.; Yang, Z. Assessing the toxicity and
19 biodegradability of deep eutectic solvents. *Chemosphere* **2015**, *132*, 63-69.
20
21 38. Alhadid, A.; Mokrushina, L.; Minceva, M. Design of deep eutectic systems: a simple
22 approach for preselecting eutectic mixture constituents. *Molecules* **2020**, *25*, No. 1077.
23
24 39. Martins, M. A.; Pinho, S. P.; Coutinho, J. A. Insights into the nature of eutectic and deep
25 eutectic mixtures. *J. Solution Chem.* **2019**, *48*, 962-982.
26
27 40. Alhadid, A.; Mokrushina, L.; Minceva, M. Modeling of solid-liquid equilibria in deep
28 eutectic solvents: a parameter study. *Molecules* **2019**, *24*, No. 2334.
29
30 41. Abbott, A. P.; Ahmed, E. I.; Prasad, K.; Qader, I. B.; Ryder, K. S. Liquid pharmaceuticals
31 formulation by eutectic formation. *Fluid Phase Equilibr.* **2017**, *448*, 2-8.
32
33 42. Klamt, A.; Eckert, F. COSMO-RS: a novel and efficient method for the a priori prediction
34 of thermophysical data of liquids. *Fluid Phase Equilibr.* **2000**, *172*, 43-72.
35
36 43. Song, Z.; Zhang, J.; Zeng, Q.; Cheng, H.; Chen, L.; Qi, Z. Effect of cation alkyl chain
37 length on liquid-liquid equilibria of {ionic liquids+ thiophene+ heptane}: COSMO-RS
38 prediction and experimental verification. *Fluid Phase Equilibr.* **2016**, *425*, 244-251.
39
40 44. Abbott, A. P.; Capper, G.; Davies, D. L.; Rasheed, R. K.; Tambyrajah, V. Novel solvent
41 properties of choline chloride/urea mixtures. *Chem. Commun.* **2003**, *1*, 70-71.
42
43 45. Guo, W.; Hou, Y.; Ren, S.; Tian, S.; Wu, W. Formation of deep eutectic solvents by
44 phenols and choline chloride and their physical properties. *J. Chem. Eng. Data* **2013**, *58*,
45 866-872.
46
47 46. Crespo, E. A.; Silva, L. P.; Martins, M. A.; Fernandez, L.; Ortega, J.; Ferreira, O.;
48 Sadowski, G.; Held, C.; Pinho, S. P.; Coutinho, J. A. Characterization and modeling of the
49 liquid phase of deep eutectic solvents based on fatty acids/alcohols and choline chloride.
50 *Ind. Eng. Chem. Res.* **2017**, *56*, 12192-12202.
51
52
53
54
55
56
57
58
59
60

- 1
2
3 47. Silva, L. P.; Fernandez, L.; Conceição, J. H.; Martins, M. A.; Sosa, A.; Ortega, J.; Pinho,
4 S. P.; Coutinho, J. A. Design and characterization of sugar-based deep eutectic solvents
5 using conductor-like screening model for real solvents. *ACS Sustain. Chem. Eng.* **2018**, *6*,
6 10724-10734.
7
8
9 48. Abranches, D. O.; Larriba, M.; Silva, L. P.; Melle-Franco, M.; Palomar, J. F.; Pinho, S. P.;
10 Coutinho, J. A. Using COSMO-RS to design choline chloride pharmaceutical eutectic
11 solvents. *Fluid Phase Equilib.* **2019**, *497*, 71-78.
12
13 49. Benguerba, Y.; Alnashef, I. M.; Erto, A.; Balsamo, M.; Ernst, B. A quantitative prediction
14 of the viscosity of amine based DESs using $\Sigma\sigma$ -profile molecular descriptors. *J. Mol.*
15 *Struct.* **2019**, *1184*, 357-363.
16
17 50. Zhou, T.; Qi, Z.; Sundmacher, K. Model-based method for the screening of solvents for
18 chemical reactions. *Chem. Eng. Sci.* **2014**, *115*, 177-185.
19
20 51. Zhang, Y.; Ji, X.; Lu, X. Choline-based deep eutectic solvents for CO₂ separation: review
21 and thermodynamic analysis. *Renew. Sustain. Energy Rev.* **2018**, *97*, 436-455.
22
23 52. Li, G.; Deng, D.; Chen, Y.; Shan, H.; Ai, N. Solubilities and thermodynamic properties of
24 CO₂ in choline-chloride based deep eutectic solvents. *J. Chem. Thermodyn.* **2014**, *75*, 58-
25 62.
26
27 53. Liu, X.; Gao, B.; Jiang, Y.; Ai, N.; Deng, D. Solubilities and thermodynamic properties of
28 carbon dioxide in guaiaicol-based deep eutectic solvents. *J. Chem. Eng. Data* **2017**, *62*,
29 1448-1455.
30
31 54. Chen, Y.; Ai, N.; Li, G.; Shan, H.; Cui, Y.; Deng, D. Solubilities of carbon dioxide in
32 eutectic mixtures of choline chloride and dihydric alcohols. *J. Chem. Eng. Data* **2014**, *59*,
33 1247-1253.
34
35 55. Leron, R. B.; Caparanga, A.; Li, M. H. Carbon dioxide solubility in a deep eutectic
36 solvent based on choline chloride and urea at T=303.15–343.15 K and moderate pressures.
37 *J. Taiwan Inst. Chem. Eng.* **2013**, *44*, 879-885.
38
39 56. Leron, R. B.; Li, M. H. Solubility of carbon dioxide in a eutectic mixture of choline
40 chloride and glycerol at moderate pressures. *J. Chem. Thermodyn.* **2013**, *57*, 131-136.
41
42 57. Leron, R. B.; Li, M. H. Solubility of carbon dioxide in a choline chloride–ethylene glycol
43 based deep eutectic solvent. *Thermochim. Acta* **2013**, *551*, 14-19.
44
45 58. Benfenati, E.; Manganaro, A.; Gini, G. C. VEGA-QSAR: AI inside a platform for
46 predictive toxicology. *CEUR Workshop Proceedings*, **2013**, *1107*, 21-28.
47
48
49
50
51
52
53
54
55
56
57
58
59
60

- 1
2
3 59. Wang, J.; Song, Z.; Cheng, H.; Chen, L.; Deng, L.; Qi, Z. Computer-aided design of ionic
4 liquids as absorbent for gas separation exemplified by CO₂ capture cases. *ACS Sustain.*
5 *Chem. Eng.* **2018**, *6*, 12025-12035.
6
7 60. Bechtel, S.; Song, Z.; Zhou, T.; Vidakovic-Koch, T.; Sundmacher, K. Integrated process
8 and ionic liquid design by combining flowsheet simulation with quantum-chemical
9 solvent screening. *Comput. Aided Chem. Eng.* **2018**, *44*, 2167-2172.
10
11 61. Perez-Salado Kamps, A.; Tuma, D.; Xia, J.; Maurer, G. Solubility of CO₂ in the ionic
12 liquid [bmim][PF₆]. *J. Chem. Eng. Data* **2003**, *48*, 746-749.
13
14 62. Aki, S. N.; Mellein, B. R.; Saurer, E. M.; Brennecke, J. F. High-pressure phase behavior
15 of carbon dioxide with imidazolium-based ionic liquids. *J. Phys. Chem. B* **2004**, *108*,
16 20355-20365.
17
18 63. Murrieta-Guevara, F.; Romero-Martinez, A.; Trejo, A. Solubilities of carbon dioxide and
19 hydrogen sulfide in propylene carbonate, N-methylpyrrolidone and sulfolane. *Fluid Phase*
20 *Equilibr.* **1988**, *44*, 105-115.
21
22 64. Gainar, I., Anitescu, G. The solubility of CO₂, N₂ and H₂ in a mixture of dimethylether
23 polyethylene glycols at high pressures. *Fluid Phase Equilibr.* **1995**, *109*, 281-289.
24
25 65. Sander, R. Compilation of Henry's law constants (version 4.0) for water as solvent. *Atmos.*
26 *Chem. Phys.* **2015**, *15*, 4399-4981.
27
28
29
30
31
32
33
34
35
36
37
38
39
40
41
42
43
44
45
46
47
48
49
50
51
52
53
54
55
56
57
58
59
60

Table 1. Statistical results of the obtained MLR for ΔT_f .

Variables	Estimated coefficients	Standard error	tStat	F	p-value
HB_don3	9.03	1.50	6.03	36.30	1.98×10^{-6}
HB_acc3	2.90	1.13	2.56	6.55	1.60×10^{-2}
V _{COSMO}	-0.23	0.03	-7.30	53.25	7.54×10^{-8}
Intercept	136.02	10.92	12.46	-	1.04×10^{-12}

Model statistics: $R^2=0.85$, adjusted $R^2=0.83$, RMSE=16.8

Table 2. Top 10 DES candidates screened according to the ranking of $AC \times DE \times 10^3$.

Ranking	HBD	ChCl: HBD	AC $\times 10^3$	DE	AC $\times DE \times 10^3$
1*	urea	1:2	2.21	1.62	3.58
2	ethylenecyanohydrin	1:1	2.33	1.49	3.46
3	ethylenecyanohydrin	1:2	2.03	1.55	3.15
4	ethylenecyanohydrin	1:3	1.90	1.56	2.96
5	pyruvicacid	1:1	1.77	1.51	2.66
6	1-(2-hydroxyethyl)imidazole	1:1	1.75	1.48	2.59
7	cyanoaceticacid	1:1	1.61	1.57	2.53
8	4-pentyn-1-ol	1:1	1.69	1.47	2.50
9	4-pentyn-1-ol	1:3	1.70	1.45	2.47
10*	ethylene glycol	1:1.75	1.57	1.53	2.40

*: DESs that have been experimentally reported.

Table 3. Comparison of the H_m of CO₂ in the studied DESs at around 298.15 K with that in previously reported DESs and typical ionic liquids.

Solvents	H_m (MPa.kg/mol)	Ref.
Propylene carbonate	0.78 ^a	63
Dimethyl ether of polyethylene glycol	1.00 ^a	64
Water	2.93 ^a	65
[Bmim][BF ₄]	0.94 ^a	62
[Bmim][TfO]	1.00 ^a	62
[Bmim][Tf ₂ N]	1.06 ^a	62
[Bmim][DCA]	1.10 ^a	62
[Bmim][PF ₆]	1.19 ^b	61
[Bmim][NO ₃]	1.60 ^a	62
ChCl: ethylenecyanohydrin (1:2)	0.99 ^a	this work
ChCl: ethylenecyanohydrin (1:3)	1.09 ^a	this work
ChCl: urea (1:2)	1.31 ^c	55
ChCl: glycerol (1:2)	1.41 ^c	56
ChCl: ethylene glycol (1:2)	1.84 ^c	57
DEHCl: guaiacol (1:5)	2.25 ^b	53
DEHCl: guaiacol (1:4)	2.33 ^b	53
ChCl: phenol (1:4)	2.38 ^b	52
DEHCl: guaiacol (1:3)	2.44 ^b	53
ChCl: phenol (1:2)	2.47 ^b	52
ChCl: phenol (1:3)	2.50 ^b	52
ChCl: triethylene glycol (1:4)	2.56 ^b	52
ChCl: triethylene glycol (1:3)	2.56 ^b	52
ChCl: 2,3-butanediol (1:4)	2.59 ^b	54
ChCl: 1,2-propanediol (1:4)	2.60 ^b	4
ACCl: guaiacol (1:5)	2.63 ^b	53
ChCl: diethylene glycol (1:4)	2.64 ^b	52
ACCl: guaiacol (1:4)	2.75 ^b	53
ChCl: 1,2-propanediol (1:3)	2.76 ^b	54
ChCl: guaiacol (1:5)	2.79 ^b	53
ACCl: guaiacol (1:3)	2.79 ^b	53
ChCl: diethylene glycol (1:3)	2.96 ^b	52
ChCl: guaiacol (1:4)	2.98 ^b	53
ChCl: guaiacol (1:3)	3.10 ^b	53
ChCl: 1,4-butanediol (1:3)	3.12 ^b	54
ChCl: 1,4-butanediol (1:4)	3.21 ^b	54
ChCl: 2,3-butanediol (1:3)	3.32 ^b	54

a. H_m at 298.15 K; b. H_m at 293.15 K; c. H_m at 303.15 K.

Figure captions

Figure 1. Systematic DES screening method proposed in this work.

Figure 2. Illustration of a typical DES phase diagram ($T_{f,A}$ and $T_{f,B}$: freezing points of individual component A and B; $T_{f,im}^*$ and $T_{f,im}$: ideally interpolated temperature at the assumed maximum and the practical eutectic composition; T_{me} and T_e : estimated maximum and the practical eutectic temperature; x_e : the eutectic composition).

Figure 3. Comparison of the experimentally determined and MLR correlated ΔT_f of ChCl-based DESs.

Figure 4. Grade table of the five EHS-relevant properties of HBDs illustrated with some representatives.

Figure 5. Comparison of experimentally determined and COSMO-RS predicted H_x of CO₂ in different DESs.

Figure 6. COSMO-RS derived AC and DE of different DESs obtained after the EHS screening.

Figure 7. Solubility of CO₂ in the prepared ChCl: ethylenecyanohydrin DESs as a function of pressure (symbols, experimental; lines, linear fit).

1
2
3 **Figure 1.** Systematic DES screening method proposed in this work.
4
5

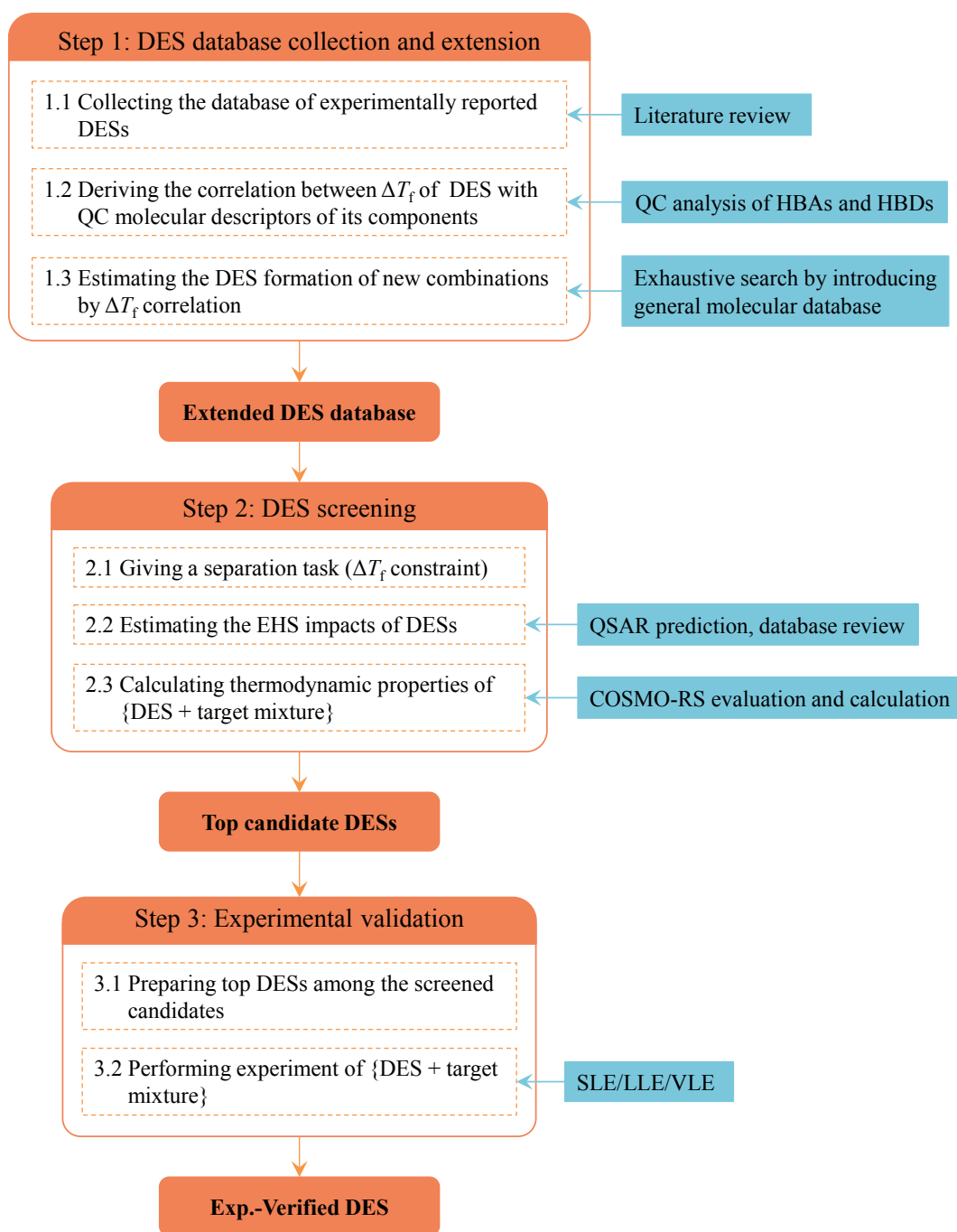


Figure 2. Illustration of a typical DES phase diagram ($T_{f,A}$ and $T_{f,B}$: freezing points of individual component A and B; T_{f,im^*} and $T_{f,im}$: ideally interpolated temperature at the assumed maximum and the practical eutectic composition; T_{me} and T_e : estimated maximum and the practical eutectic temperature; x_e : the eutectic composition).

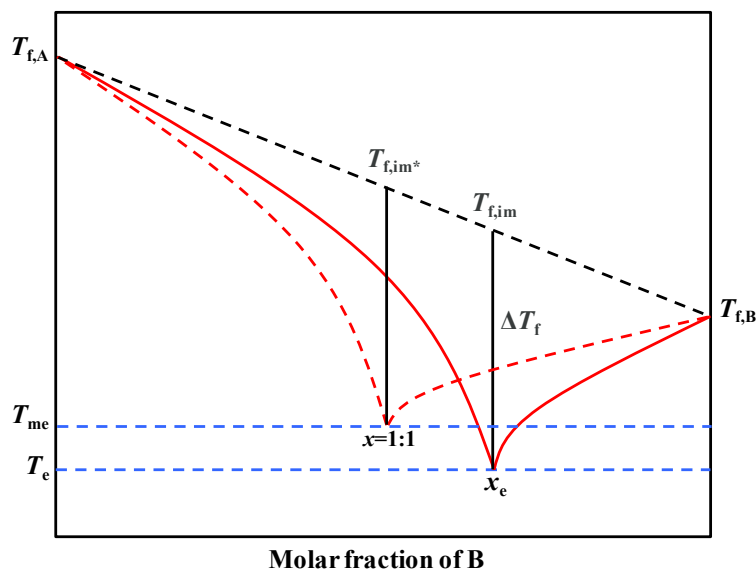


Figure 3. Comparison of the experimentally determined and MLR correlated ΔT_f of ChCl-based DESs.

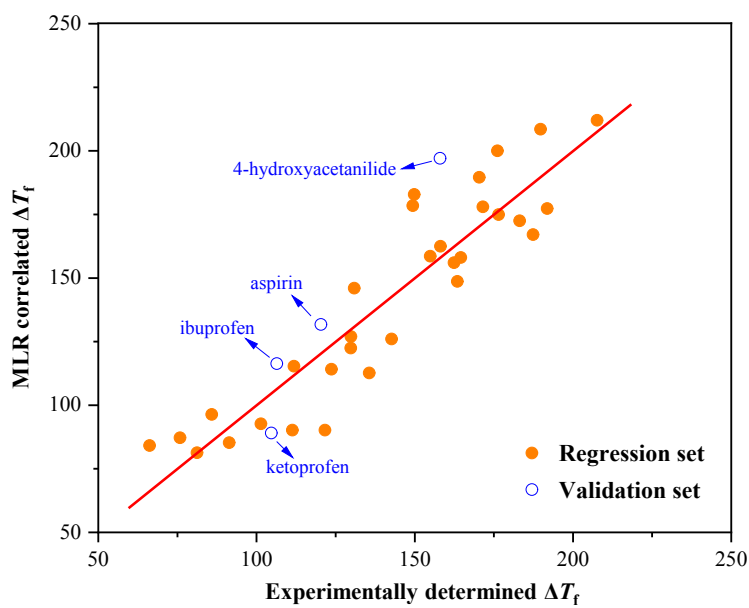


Figure 4. Grade table of the five EHS-relevant properties of HBDs illustrated with some representatives.

	Persistence	BCF	Mutagenicity	Carcinogenicity	Toxicity
1,2,4-triazole	Yellow	Purple	Purple	Yellow	Purple
2-bromoethanol	Purple	Green	Red	Red	Blue
2-furanmethanol	Purple	Purple	Green	Red	Yellow
3-butyn-2-ol	Purple	Green	Blue	Blue	Red
3-chloro-1-propanol	Green	Green	Red	Blue	Blue
3-fluorophenol	Purple	Green	Purple	Blue	Red
acetaldehydroxime	Purple	Purple	Green	Green	Red
acetic acid	Green	Green	Green	Blue	Green
butyraldoxime	Purple	Purple	Blue	Yellow	Blue
D-(+)-glucose	Green	Purple	Blue	Blue	Blue
ethylenecyanohydrin	Purple	Green	Green	Green	Blue
glycerol	Green	Green	Green	Green	Green
glyoxylicacid	Green	Purple	Green	Blue	Red
hydroxyurea	Yellow	Purple	Red	Yellow	Yellow
imidazole	Purple	Purple	Green	Blue	Yellow
methacrylicacid	Green	Green	Green	Blue	Red
methylimidazole	Yellow	Purple	Green	Green	Yellow
methylphosphonicacid	Purple	Purple	Yellow	Green	Yellow
phenol	Green	Green	Green	Green	Red
propynol	Purple	Purple	Red	Green	Red
pyrrole	Purple	Purple	Green	Blue	Green
pyruvicacid	Green	Green	Green	Green	Blue
thiolacticacid	Purple	Purple	Green	Green	Yellow
urethane	Green	Green	Yellow	Red	Green

Figure 5. Comparison of experimentally determined and COSMO-RS predicted H_x of CO_2 in different DESs.

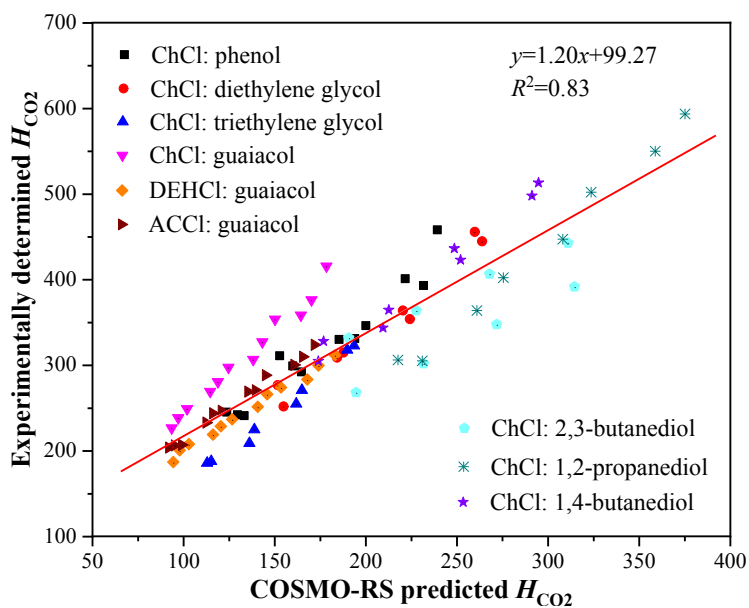


Figure 6. COSMO-RS derived AC and DE of different DESs obtained after EHS screening.

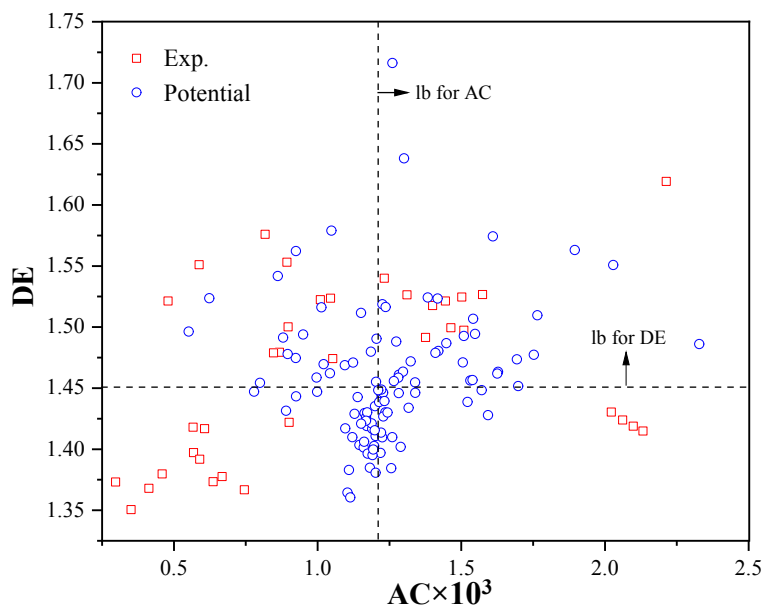


Figure 7. Solubility of CO₂ in the prepared ChCl: ethylenecyanohydrin DESs as a function of pressure (symbols, experimental; lines, linear fit).

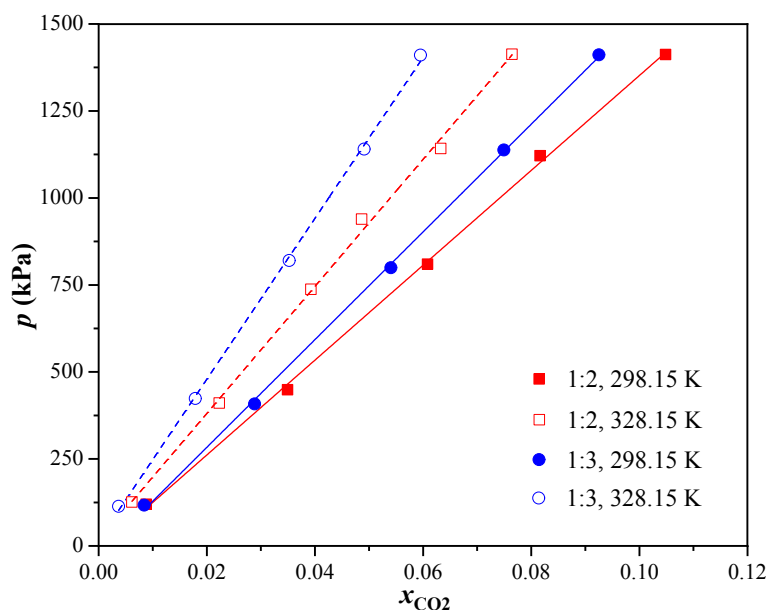
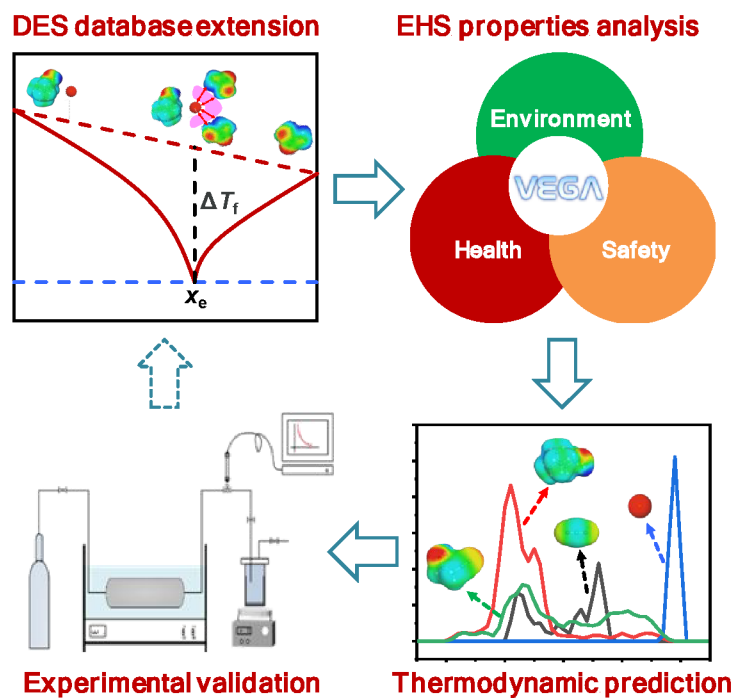


Table of Contents



Synopsis: Rationally screened deep eutectic solvents possess great potential as efficient and sustainable media for various separation process.